

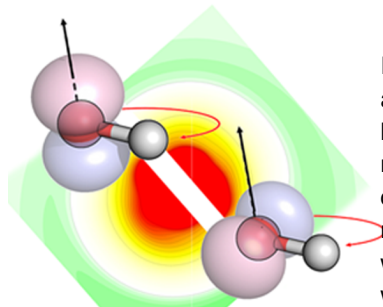
Product lambda-doublet ratios for the $O(^3P) + D_2$ reaction: A mechanistic imprint.

P. G. Jambrina,^a A. Zanchet,^a J. Aldegunde,^b M. Brouard,^c and F. J. Aoiz^{*a}

^a Departamento de Química Física I, Universidad Complutense de Madrid, Spain.

^b Departamento de Química Física, Universidad de Salamanca, Spain.

^c The Department of Chemistry, University of Oxford, United Kingdom



In the last decade, the development of theoretical methods have allowed chemists to reproduce and explain almost all of the experimental data associated with elementary atom plus diatom collisions. However, there are still a few examples where theory cannot account yet for experimental results. This is the case for the preferential population of one of the Λ -doublet states produced by chemical reactions. In particular, recent measurements of the $OD(^2\Pi)$ product of the $O(^3P) + D_2$ reaction have shown a clear preference for the $\Pi(A')$ Λ -doublet states, in apparent contradiction with *ab initio* calculations, which predict a larger reactivity on the A'' potential energy surface. Here we present a method to calculate the Λ -doublet ratio when concurrent potential energy surfaces participate in the reaction. It accounts for the experimental Λ -doublet populations via explicit consideration of the stereodynamics of the process. Furthermore, our results demonstrate that the propensity of the $\Pi(A')$ state is a consequence of the different mechanisms of the reaction on the two concurrent potential energy surfaces.

1 Introduction

Chemists are keen to describe chemical reactions in terms of the motion of billiard balls on a more or less complex quantum electronic landscape, the Potential Energy Surface (PES). However, this picture is not always valid and quite often, several PESs have to be considered, giving rise to non-adiabatic effects that may have a decisive influence on the dynamics. When this is the case, it is not possible to disentangle experimentally the contribution of each of the competing surfaces, answering the question of which of them is more/less reactive, and why. The presence of multiple PESs correlating reactants and products leads to open shell molecules in which the rotational levels are split in spin-orbit states, and, in turn, each of them in two nearly degenerate Λ -doublet levels that can be spectroscopically resolved due to different selection rules. In spite of the tiny energy difference between the Λ -doublet pair of states, a clear preference towards one of them is observed in many chemical reactions¹⁻⁶. As pointed out by several authors,⁷⁻¹⁶ the Λ -doublet population acts as a fingerprint to unravel the symmetries of the surfaces involved in the process so that the propensity for one of the manifolds reflects the competing reactivity of concurrent PESs and addresses the question of where the electrons go when the reaction takes place^{14,16}. However, a general, clear-cut relationship between them has not yet been demonstrated.

Collisions leading to $NO(^2\Pi)$ and $OH(^2\Pi)$ are prototypical for the study of Λ -doublet propensities. Recent experiments by Minton, McKendrick and coworkers^{5,6} have determined the $OD(X^2\Pi)$ state-to-state Λ -doublet population ratios for $O(^3P) + D_2$ collisions. Regardless of the collision energy and final vibrational

state, they consistently found a significantly larger population of the $\Pi(A')$ Λ -doublet state compared to the $\Pi(A'')$ one, where the labelling of the states refers to the location of the singly occupied orbital in the rotation plane of the diatom, $\Pi(A')$, or perpendicular to it, $\Pi(A'')$, in the limit of high products rotational states j' .^{13,15,17} This result seems to contradict the theoretical results, which would predict a preference for $\Pi(A'')$ under the assumption that for the two concurrent PESs, of symmetry $^3A'$ and $^3A''$, collisions on the first one will only form the $\Pi(A')$ Λ -doublet state and vice-versa. This simple assignment is supported by the rationale that for direct, sudden collisions, the products “remember” the collision conditions and, thus, there should be a close relationship between both symmetries. It should be pointed out that a general procedure to connect the reactivity on concurrent surfaces with the Λ -doublet population has not been achieved. In what follows, we present a method that connects the reactivity on the A' and A'' PESs with the populations of the respective Λ -doublet states, through the explicit consideration of the reaction stereodynamics. As will be shown, this method is capable to reproduce and to explain the origin of the experimental Λ -doublet propensities.

This article is organized as follows: In the theory section we will present the method (the interested reader is referred to the Appendix for a more detailed presentation). In the Results and Discussion section, the $OD(X^2\Pi)$ Λ -doublet population ratios for $O(^3P) + D_2$ reaction have been calculated and compared with the experimental results. The present theory also allows us to connect the predicted Λ -doublet propensities with the reaction mechanism. Finally, the main conclusions will be summarized.

*E-mail: aoiz@quim.ucm.es

2 Theory

We will start by invoking conservation of the reactive flux, which implies that the population of the two Λ -doublet states and the cross sections on the A' and A'' PESs are related by

$$\sigma_{v'j'}(\Pi(A')) = W_{A'} \sigma_{v'j'}(A') + (1 - W_{A''}) \sigma_{v'j'}(A'') \quad (1)$$

$$\sigma_{v'j'}(\Pi(A'')) = (1 - W_{A'}) \sigma_{v'j'}(A') + W_{A''} \sigma_{v'j'}(A''), \quad (2)$$

where $\sigma_{v'j'}(A')$ and $\sigma_{v'j'}(A'')$ are the rovibrational state resolved cross sections on the two respective PESs and $W_{A'}$ and $W_{A''}$ represent the ‘‘correction factors’’ to obtain the Λ -doublet cross sections for a given v', j' rovibrational state. As commented on above, in the sudden limit, the flux ending on the A' PES is assigned to the $\Pi(A')$ state and *vice versa*, which is equivalent to setting $W_{A'} = 1$, and $W_{A''} = 1$.

For a given nuclear geometry, the weights $W_{A'}$ and $W_{A''}$ are the square of the coefficients that define the expansion of the D–OD asymptotic electronic wavefunctions in terms of the Λ -doublet molecular wavefunctions $\varphi[\Pi(A')]$ and $\varphi[\Pi(A'')]$,¹⁴

$$\psi_{A'} = \alpha_1^{A'} \varphi[\Pi(A')] + \alpha_2^{A'} \varphi[\Pi(A'')] \quad (3)$$

$$\psi_{A''} = \alpha_1^{A''} \varphi[\Pi(A')] + \alpha_2^{A''} \varphi[\Pi(A'')] \quad (4)$$

These coefficients are related to the dihedral angle between the three-atom plane and the OD molecular plane.¹⁴ This angle connects the symmetry of the PES to that of the Λ -doublet state, and, in the high j' limit, can be identified with $\theta_{j'\mathbf{u}}$, the angle between the rotational angular momentum, \mathbf{j}' , perpendicular to the OD rotation plane and the vector \mathbf{u} perpendicular to the three-atom plane¹⁸ (see Fig. 6 in the Appendix). For the A' PES the singly occupied orbital lies in the triatomic plane and, hence, $\alpha_1^{A'} = \cos \theta_{j'\mathbf{u}}$, and $\alpha_2^{A'} = \sin \theta_{j'\mathbf{u}}$. Conversely, for the A'' PES, the orbital lies perpendicular to the triatomic plane, leading to $\alpha_1^{A''} = -\sin \theta_{j'\mathbf{u}}$, and $\alpha_2^{A''} = \cos \theta_{j'\mathbf{u}}$.

To obtain the weights $W_{A'}$ and $W_{A''}$, one just needs to average $\cos^2 \theta_{j'\mathbf{u}}$ over one rotational period for calculations on the A' and A'' PES respectively. This is straightforward in the quasiclassical trajectories (QCT) framework,¹⁸ where $\theta_{j'\mathbf{u}}$ can be computed at every step of the trajectory. In a pure quantum mechanical (QM) context the equivalent magnitude would be $\langle j'^2_{\mathbf{u}} \rangle / (j'(j+1))$, where $j'^2_{\mathbf{u}}$ is the projection of the rotational angular momentum along the \mathbf{u} vector.

A crucial finding, that can be demonstrated using either QCT or QM arguments (see Appendix), is that $\langle \cos^2 \theta_{j'\mathbf{u}} \rangle_{\text{rot}}$, the average value of the square angle cosine is related to the helicity, Ω' , the projection of \mathbf{j}' on the products recoil direction (\mathbf{k}'), through the expression:

$$\langle \cos^2 \theta_{j'\mathbf{u}} \rangle_{\text{rot}} = 1 - \left| \frac{\Omega'^2}{j'(j'+1)} \right|^{1/2}, \quad (5)$$

Equation (5) has very important implications: $W_{A'}$ and $W_{A''}$ for a given rovibrational state depend only on the distribution of the helicities and, in general, will differ because such distributions reflect the mechanisms on the concurrent PESs, that can be different. This means that equations (1) to (5) can be used to: i)

determine Λ -doublet populations also in a purely QM context, for which Ω' is well defined, and ii) relate the Λ -doublet populations with the reaction mechanism (see below).

The average value of $|\Omega'|^2$ can be determined from the product rotational alignment moment, $a_0^{(2)}(j')$, which contains the essential information about the alignment of \mathbf{j}' with respect to the product recoil velocity, and is given by¹⁹

$$a_0^{(2)}(j') = \frac{\sum \sigma_{v'j'}(\Omega') \langle j'\Omega', 20 | j'\Omega' \rangle}{\sigma_{v'j'}} = \frac{\sum \sigma_{v'j'}(\Omega') [3\Omega'^2 - j'(j'+1)]}{2C \sigma_{v'j'}}, \quad (6)$$

where $\sigma_{v'j'}(\Omega')$ is the cross section resolved in (v', j', Ω') , $\langle \cdot, 20 | \cdot \rangle$ is the Clebsch-Gordan coefficient. $C = [j'(j'+1)(j'-1/2)(j'+3/2)]^{1/2}$, which for high enough j' is $\approx j'(j'+1)$. The average value of Ω' for a given j' is

$$\langle \Omega'^2 \rangle = \frac{\sum \sigma_{v'j'}(\Omega') \Omega'^2}{\sigma_{v'j'}} = \frac{2C a_0^{(2)}(j')}{3} + \frac{j'(j'+1)}{3}, \quad (7)$$

leading to the following expression for $W_{A'}$,

$$W_{A'} = 1 - \left[\frac{\langle \Omega'^2 \rangle}{j'(j'+1)} \right]^{1/2} \approx 1 - \left[\frac{2}{3} a_0^{(2)}(j') + \frac{1}{3} \right]^{1/2}, \quad (8)$$

where the polarization moments, $a_0^{(2)}(j')$, have been calculated on the A' PES. Identical expressions hold for $W_{A''}$ when the $a_0^{(2)}$ alignment moment is calculated on the A'' PES are used. Equation. (8) has one important consequence: *the stereodynamics of the products - specifically, the \mathbf{k}' - \mathbf{j}' correlation - relates the Λ -doublet populations to the reactivity on the A' and A'' PESs*. Classically, $a_0^{(2)}$ lies in the $[-1/2, 1]$ range, although its QM limiting values depends on j' . Negative values of $a_0^{(2)}$, close to its lower limit, correspond to $\mathbf{j}' \perp \mathbf{k}'$ and $|\Omega'| \approx 0$, whilst positive values, close to one, imply that $\mathbf{j}' \parallel \mathbf{k}'$ and $|\Omega'| \approx j'$. According to eqn (8), weight factors close to zero are associated with $a_0^{(2)} \approx 1$; that is, products on the A' PES would appear as the $\Pi(A'')$ Λ -doublet state and *vice versa*. When $a_0^{(2)} \approx -1/2$, the weight factor tends to 1 and products on the A' PES would correspond to the $\Pi(A')$ Λ -doublet state.

3 Results and Discussion

Aiming to test the method and to try to reproduce the experimental results of Minton, McKendrick and coworkers^{5,6}, we carried out adiabatic time-independent QM and QCT calculations following the procedures described in Refs. 20–22 using a new set of $^3A'$ and $^3A''$ PESs (see method section for further details).

The adiabatic QM state-to-state reactive cross sections for the $O(^3P) + D_2$ reaction at $E_{\text{coll}} = 25 \text{ kcal mol}^{-1}$, one of the energies of the experiments carried out by Minton and coworkers⁵, are represented on the top left panel of Fig. 1. These results show that, whilst for low OD ($v' = 0, j'$) rovibrational states the A' PES is as reactive as the A'' one, for $j' > 12$ the integral cross sections (ICS) on the A'' PES are considerably larger than those on the A' PES. This is not surprising as, although both PESs have the same barrier height, the potential energy raises faster with the bending angle for the A' electronic state than for the A'' state²³, *i.e.*,

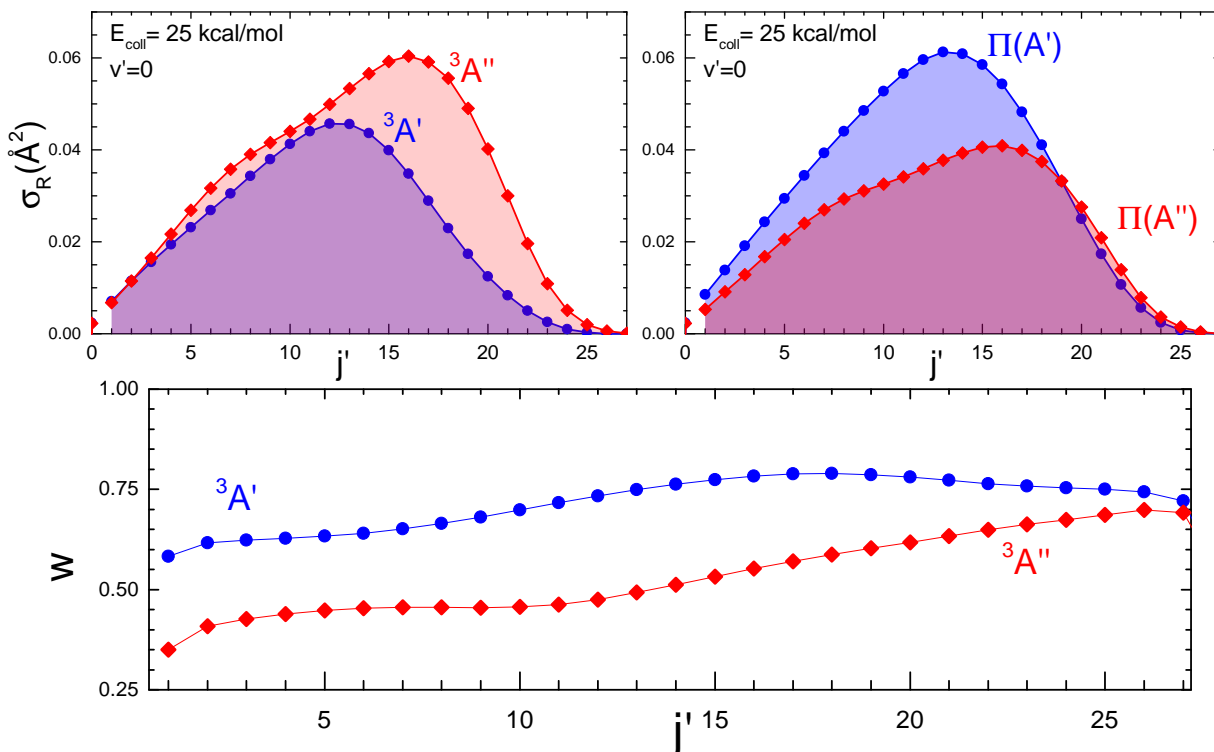


Fig. 1 QM weight factors to determine the $\Pi(A'')$ and $\Pi(A')$ populations from the integral cross section of the $3A'$ and $3A''$ PES. The top left panel displays the reactive cross sections calculated on the A' and A'' PES, which, in the sudden limit, would represent the $\Pi(A')$ and $\Pi(A'')$ state resolved cross sections. The top right panel shows the reactive cross sections calculated for the two Λ -doublet levels once respective weights have been incorporated. The weights are shown in the bottom panel. The data were obtained from the QM reaction cross sections for the $\text{O}(^3P) + \text{D}_2$ reaction at $E_{\text{coll}} = 25 \text{ kcal mol}^{-1}$.

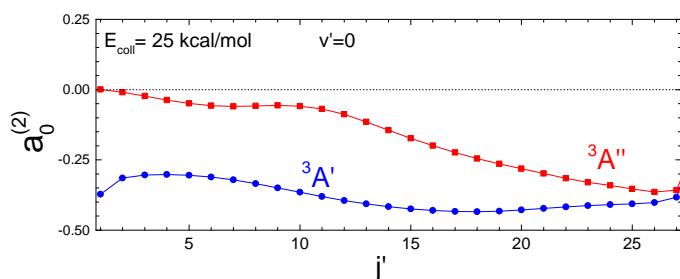


Fig. 2 Product QM alignment parameter, $a_0^{(2)}$, referenced to \mathbf{k}' (which defines the z axis). The alignment moment $a_0^{(2)}$ is given by the average value $C^{-1}(3\hat{j}_z^2 - \hat{j}^2)/2$, where \hat{j}^2 and \hat{j}_z are the rotational angular momentum operators and C is the constant that appears in eqn (6). Calculations are presented for $\text{O}(^3P) + \text{D}_2(v=0, j=0) \rightarrow \text{OD}(v'=0, j') + \text{D}$ at $E_{\text{coll}} = 25 \text{ kcal mol}^{-1}$ on the A' and A'' PESs. Whilst the product rotational angular momentum, j' , on the A' PES is strongly polarized perpendicular to \mathbf{k}' (negative $a_0^{(2)}$ values), for the A'' PES the distribution of j' is largely isotropic for low j' .

the “cone of acceptance” is larger on the A'' PES. The inclusion of non-adiabatic couplings in the dynamics does not change this picture, as trajectory surface hopping²⁴ and non-adiabatic QM calculations^{25,26} also indicate larger reactivities on the A'' PES.

Before discussing the other panels of Fig. 1, it is pertinent to inspect the integral alignment moments, $a_0^{(2)}$, which are shown in Fig. 2 as a function of the rotational state for $v' = 0$. The dif-

ferences between the values and the trends in $a_0^{(2)}(j')$ on the two PESs are conspicuous, and indicate that very different stereodynamics are at play on the two surfaces. For reaction on the A' PES, j' is strongly polarized perpendicular to the recoil direction, \mathbf{k}' , for essentially all j' states, and in some instances ($j' = 15-17$) the $a_0^{(2)}$ values are very close to the limiting negative value. In stark contrast, on the A'' PES, j' is almost unpolarized for $j' \leq 15$, with small $a_0^{(2)}$ values close to the isotropic limit, $a_0^{(2)} = 0$. With increasing j' above 15, $a_0^{(2)}$ becomes gradually more negative approaching the values found on the A' PES.

Inserting the values of the alignment moments calculated on both PESs into eqn (8) yields the weight factors, $W_{A'}$ and $W_{A''}$. They are shown in the bottom panel Fig. 1 for $v' = 0$ at $E_{\text{coll}} = 25 \text{ kcal mol}^{-1}$. As can be seen, for $j' < 15$, $W_{A''} < 0.5$, which, in effect, means that more than 50% of the reactivity on the A'' PES is “transferred” to the $\Pi(A')$ Λ -doublet state. In contrast, as a result of the consistently fairly negative values of the alignment parameters, $W_{A'}$ is always > 0.6 and in some cases is as large as 0.80. In consequence, the relative “transfer” of reactivity from A' to $\Pi(A'')$ is much less significant than that found from A'' to $\Pi(A')$.

Therefore, after correction, the relative population on the $\Pi(A')$ state is significantly enhanced. The resulting Λ -doublet populations are depicted in the right panel of Fig. 1. Quite remarkably, the situation is the reverse of that found for the reactivity on the respective PESs: the $\Pi(A')$, Λ -doublet state is considerably

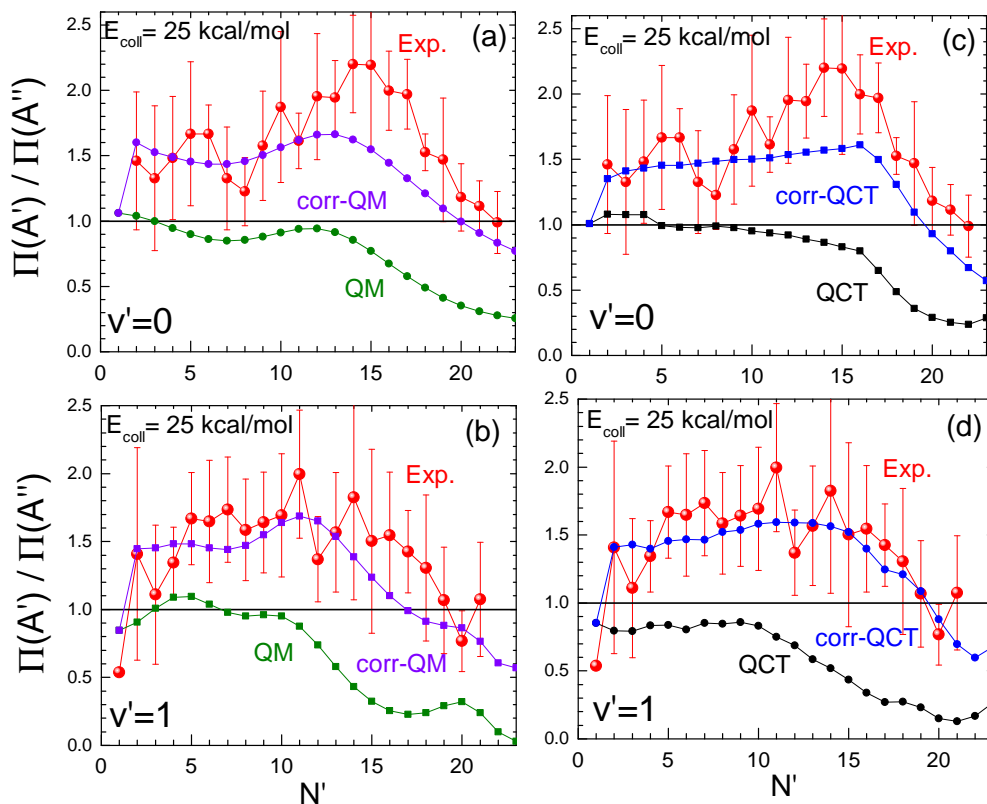


Fig. 3 Experimental (from Ref. 5), and the present QCT and QM Λ -doublet population ratios for the $O(^3P) + D_2$ reaction at $E_{\text{coll}} = 25 \text{ kcal mol}^{-1}$. 'QM' and 'QCT' represent the ICSs obtained on the A' and A'' PES without any correction factor, whereas 'corr-QM' and 'corr-QCT' are the $\Pi_{A'}/\Pi_{A''}$ ratios after making use of the respective weight factors.

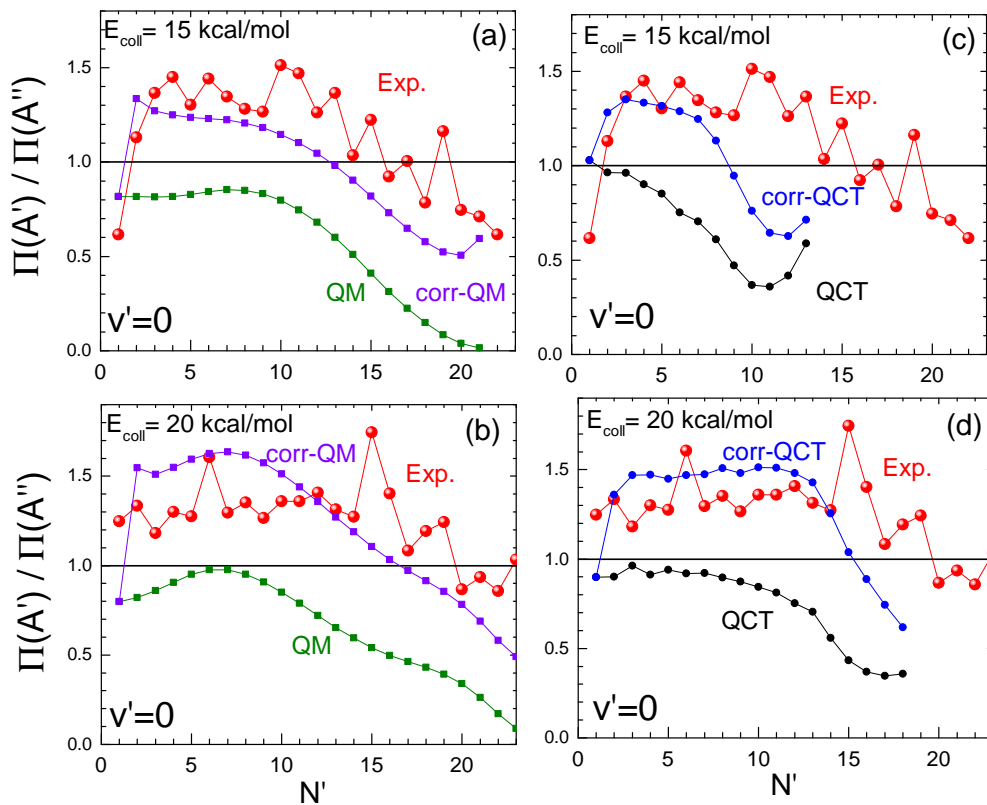


Fig. 4 Experimental, QCT, and QM Λ -doublet ratios for the $O(^3P) + D_2$ reaction at $E_{\text{coll}} = 15, 20 \text{ kcal mol}^{-1}$. The experimental error bars were not reported at Ref. 6.

more populated than the $\Pi(A'')$ state for low j' . In particular, for $j' = 12$, $\sigma(\Pi_{A''}) = (3/2) \times \sigma(\Pi_{A'})$. At higher j' values ($j' > 18$) the populations of the two Λ -doublets are very similar.

In Fig. 3, the experimental Λ -doublet population ratios measured⁵ at 25 kcal mol⁻¹ are compared with the present QM (left panels) and QCT (right panel) calculations for the $v' = 0, 1$ manifolds. All the results are plotted against $N' = j' + 1$, where j' and N' stand for the nuclear (closed-shell) and total (apart from spin) rotational angular momentum, respectively. For each case, two series of results are shown: (i) the ratio of the ICSs on the A' and A'' (labeled as 'QCT' and 'QM') where $W_{A'}$ and $W_{A''}$ are implicitly set to one, and (ii) the ratio of the populations on the $\Pi(A')/\Pi(A'')$ using eqns. (1) and (2) with the correction factors included. For the latter results (labeled as 'corr-QM' and 'corr-QCT'), the $W_{A'}$ and $W_{A''}$ factors are calculated according to eqn (8). It is evident that the uncorrected QCT and QM results cannot account for the experimental Λ -doublet ratios and, regardless of j' , predict larger populations on the $\Pi(A'')$ state, in striking disagreement with the experimental results. In contrast, the corrected results reproduce fairly well the experimental values. In particular, the 'corr-QM' results are within the experimental error bars for most of the final states shown, particularly for OD ($v' = 1$).

As shown in Fig. 4, similar agreement between experimental⁶ and theoretical results is obtained at $E_{\text{coll}} = 20$ kcal mol⁻¹. At even lower collision energies, $E_{\text{coll}} = 15$ kcal mol⁻¹, the agreement between the corrected QCT and experimental results is not as good, probably because the collision energy is just above the barrier. In fact, no trajectories were found for $N' > 13$, whilst the QM and experimental data populate up to $N' = 21$. The corrected QM results remain in good agreement with the experiments at this low collision energy. It is worth noticing that while our corrected results predict quantitatively the experimental Λ -doublet ratio regardless of the collision energy and vibrational manifold studied, uncorrected results fail to account qualitatively the experimental measurements, predicting a preference towards the $\Pi(A'')$ states.

As already discussed, the way in which cross sections on the A' and A'' PESs are combined to obtain the $\Pi(A')$ and $\Pi(A'')$ populations is strictly related to the alignment of the product rotational angular momentum with respect to the recoil direction. To show this effect more clearly, the values of $\sigma(v' = 0, j', \Omega')$ as a function of Ω' and j' are depicted as contour maps in Fig. 5 for the A' and A'' PESs. The differences between the respective contour maps are clear to see. The ICS for a given j' state includes the contribution from many Ω' values on the A'' PES, whilst on the A' the contribution is restricted to relatively few, low Ω' values. Hence, this picture complements Fig. 2. Negative values of $a_0^{(2)}$ close to the limit imply that $\langle |\Omega'| \rangle$ is very small, nearly zero. If the contributions of higher Ω' values becomes more significant, the alignment moment tends to be zero.

A more quantitative analysis can be carried out by relating the Ω' contributions to the weight factors that have been used to extract the Λ -doublet populations. To this end, we have used iso-contour lines for the different values of the weight factors. If in eqn (8), $a_0^{(2)}$ is replaced with the $\langle j' \Omega', 20 | j' \Omega' \rangle$, which is nothing but the $a_0^{(2)}$ for a pure (j', Ω') state, we can assign a single

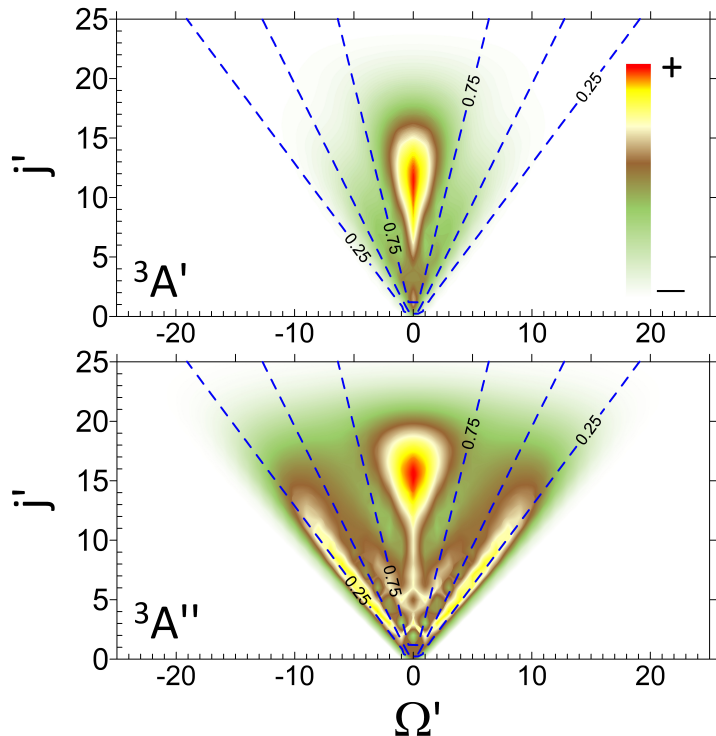


Fig. 5 Contour plots of the Ω' -resolved QM cross sections, $\sigma(v' = 0, j', \Omega')$, at $E_{\text{coll}} = 25$ kcal mol⁻¹ calculated on the A' PES (top panel), and on the A'' PES (bottom panel) as a function of both $|\Omega'|$ and j' . The contour lines indicate the values of $W_{A'}$ and $W_{A''}$ for a given combination of j' and $|\Omega'|$.

weight factor to every point on the $j' - \Omega'$ surface. On the A' PES, most of the reactivity comes from low Ω' values ($j' \perp k'$), falling within the $W_{A'} > 0.75$ limits shown by the central dashed lines in Fig. 5. In contrast, on the A'' PES we find two different trends. For the highest j' values ($j' > 15$) most of the reactivity corresponds to low Ω' , as for the A' PES, although some contributions from higher Ω' values can also be seen. However, with decreasing j' , the low Ω' peak coexists with additional peaks corresponding to $\Omega' \approx j'$ values ($j' \parallel k'$), which appear along the $W_{A''} \approx 0.25$ dashed lines. The averaging over these two contributions leads to a nearly isotropic alignment ($a_0^{(2)} \sim 0$). These contributions represent two distinct mechanisms: one coplanar which gives rise to low Ω' , and another one, that takes place only on the A'' PES, which correlates with high Ω' states and for which the three-atom and OD rotational plane tend to be orthogonal.

4 Conclusions

In spite of the tiny energy difference between the Λ -doublet pair of states, a clear preference towards a particular Λ -doublet state is observed for many chemical reactions. This intriguing fact has long puzzled researchers and, actually, has been the subject of an ongoing discussion for more than thirty years.

Throughout this article we have presented a new method that allows one to extract the Λ -doublet populations from the cross sections on the A' and A'' PESs. It is shown that the transformation between the reactivities on the A' and A'' PESs and the

Λ -doublet populations only requires knowledge about the stereodynamics of the reaction, in particular of the alignment of the products rotational angular momentum, j' , along the recoil direction, k' . This procedure is in principle general and can be used in combination with scattering data obtained using both QCT and QM adiabatic and non-adiabatic methods.

This method has been applied to the $O(^3P) + D_2$ reaction, for which we have carried out QCT and QM adiabatic calculations. Although couplings between the concurrent PES has not been included, our method accounts quantitatively for the experimental Λ -doublet populations obtained by Minton and coworkers^{5,6} that have thus far remained unexplained. The analysis of the results has shown that the preference for the $\Pi(A')$ Λ -doublet state is due to the existence of an additional mechanism on the A'' PES for which OD rotational plane tend to be orthogonal to the three-atom plane. This mechanism has been traced back to the comparative topographies of the A' and A'' PES, the latter characterized by a broader cone of acceptance.

5 Computational Methods

5.1 Ab Initio Calculations:

The PESs of the lowest $1^3A'$ and $1^3A''$ states were determined using 3500 *ab initio* points for each PES that were calculated using the MOLPRO suite of programs.^{27,28} For both oxygen and hydrogen atoms, an aug-cc-pV5Z basis set including *spdfg* basis functions was used. To obtain an accurate and homogeneous description of the PESs, the state-average complete active space (SA-CASSCF) method²⁹ was employed. The active space considered consisted of 8 electrons distributed in 6 orbitals ($2-6a'$ and $1a''$) in order to include all valence orbitals of oxygen and the $1s$ orbitals from both hydrogen atoms. The state-average orbitals and multireference configurations obtained were then used to calculate both the lowest $1^3A'$ and the lowest $1^3A''$ state energies with the internally contracted multireference configuration interaction method (icMRCI), including single and double excitations³⁰ and the Davidson correction.³¹

The *ab initio* icMRCI+Q energies for the $1^3A'$ and $1^3A''$ electronic states were fitted separately using the GFIT3C procedure introduced in Refs. 32–34, in which the global PES is represented by a many-body expansion:

$$V_{ABC} = \sum_A V_A^{(1)} + \sum_{AB} V_{AB}^{(2)}(r_{AB}) + V_{ABC}^{(3)}(r_{AB}, r_{AC}, r_{BC}), \quad (9)$$

where $V_A^{(1)}$ represents the energy of the atoms ($A=O,H,H$) in the ground electronic state, $V_{AB}^{(2)}$ the diatomic terms ($AB=OH,OH,HH$) and $V_{ABC}^{(3)}$ the 3-body term ($ABC=OHH$). The overall rms error of the two analytical potentials calculated over the 3500 geometries was found to be 0.61 kcal/mol and 0.44 kcal/mol for the $1^3A'$ and $1^3A''$ states, respectively.

Both PESs do not present any minimum out of the asymptotic channels, and both show two saddle points. The first saddle-point corresponds to the reaction barrier, with an energy 13.8 kcal/mol above the reactant valley. It corresponds to an O-H-H linear geometry where both states are degenerate. In both PESs, this saddle-point was found at $r_{OH} = 2.28$ a.u. and $r_{HH} = 1.71$ a.u.,

in good agreement with the position and energy of the saddle point optimized at the *ab initio* level, which is found at an r_{OH} distance of 2.30 a.u. and an r_{HH} distance of 1.68 a.u., and have an energy of 13.6 kcal/mol above entrance channel. The second saddle-point is found for a linear H-O-H geometry with both OH distances equal to 1.75 a.u., and lies at 80.7 kcal/mol above the entrance channel, well above the largest energy considered in this work.

5.2 Dynamical Calculations

Based on the PESs obtained, QCT and time independent QM calculations were carried out at the three collision energies: 15 kcal mol⁻¹, 20 kcal mol⁻¹, and 25 kcal mol⁻¹. QCT calculations consisted of batches of 5×10^6 trajectories following the methodology described in Refs. 21 and 22. The trajectories were started and finished at a atom-diatom distance of 20 a.u. ($\sim 10 \text{ \AA}$), and the integration step size was chosen to be 0.05 fs, which guarantees a energy conservation better than a 0.01%. The rovibrational energy of the reactant D_2 molecule was calculated by semiclassical quantization of the action using the potential given by the asymptotic reactant valley of the PES. The assignment of the product quantum numbers was carried out by equating the square of the classical D_2 molecule rotational angular momentum to $j'(j'+1)\hbar^2$. The vibrational quantum number v' was found by equating the internal energy of the products to a rovibrational Dunham expansion. The ‘‘quantum numbers’’ so obtained were rounded to the nearest integer.

To extract the contributions of each trajectory to the $\Pi(A')$ or $\Pi(A'')$ Λ -doublet states, it is sufficient to determine the classical product $a_0^{(2)}$ polarization parameters with respect to the recoil direction on each PES. This polarization parameter is given by $\langle P_2(\cos \theta_{j'k'}) \rangle$, where the brackets indicate the averaging over the set of reactive trajectories leading to a given final state.

Time independent QM calculations were carried out using the ABC²⁰ code. The basis set for the calculations included all the diatomic energy levels up to 63.4 kcal/mol. The propagation was carried out in 150 log-derivative sectors up to a distance of 20 a.u. For $J > 0$ the value of Ω_{\max} , the maximum value of the projection of J , and the rotational angular momentum onto the body fix axis was always chosen to be larger than the maximum value of j' energetically accessible.

Acknowledgement

The authors acknowledge funding by the Spanish Ministry of Science and Innovation (grants CTQ2012-37404-C02, CTQ2015-65033-P, and Consolider Ingenio 2010 CSD2009-00038). MB gratefully acknowledges the support of the UK EPSRC (via Programme Grant EP/L005913/1). PGJ acknowledges the Spanish Ministry of Economy and Competitiveness for the Juan de la Cierva fellowship (IJCI-2014-20615).

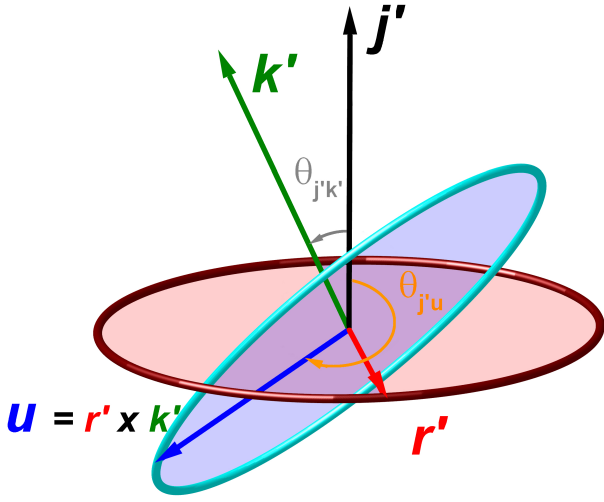


Fig. 6 The frame of coordinates that defines the various vectors relevant in the quasiclassical description. The rotational angular momentum, j' , is shown in black and kept fixed along the z axis. The O-H internuclear axis (r' , in red) rotates perpendicular to j' and its possible values are shaded in red. The recoil direction k' , also fixed, is shown as a green arrow. Vectors k' and r' define the three-atom plane. The possible directions of the vector $u = r' \times k'$ are shaded in blue. For a particular r' (red vector), u is shown as a blue arrow.

6 Appendix

6.1 Classical and Semiclassical Deduction of Equation (5)

As pointed out in the main text, the A' or A'' electronic symmetry of the potential energy surfaces is defined with respect to the rotating body-fixed DOD plane, defined by r' and R' (OD internuclear vector and the atom-diatom D-OD vector, respectively). In turn, the symmetry of the Λ -doublet states is defined with respect to the reflection in the OD rotation plane that contains r' and is perpendicular to j' , the nuclear rotational angular momentum.

Therefore, the relevant angle is $\theta_{j'u}$; that is, the angle between j' and u , a vector in the direction of $r' \times R'$. The vector R' is asymptotically parallel to the product recoil vector k' and hereinafter we will use the latter as reference. In fact, $\theta_{j'u}$ represents the dihedral angle between the molecular plane, and the three-atom plane. As pointed out in Refs. 14,18, $\cos^2 \theta_{j'u}$ can be used to relate the symmetry of the Λ -doublet levels to the symmetry of the potential energy surface (PES).

The use of $\cos^2 \theta_{j'u}$ stems from the fact that represents the probability that for each PES, the OD molecule will be produced in a given Λ -doublet state. Classically, the use of the square of the cosine of $\theta_{j'u}$ can be justified as we are interested in the mutual alignment of the planes depicted in Fig. 6.

Without any loss of generality, we can select a space-fixed (scattering) frame of coordinates in which both the product rotational angular momentum, j' , and the recoil direction, k' , are fixed. Let us also assume that j' lies along the z axis (see Fig. 6), and k' is contained in the xz plane. With this choice, the OD internuclear axis, r' , will lie in the xy plane. Then, $\theta_{k'j'}$, the angle between j' and k' , is given by:

$$\cos \theta_{k'j'} = \frac{k'_z}{|k'|}, \quad (10)$$

where k'_z is the z component of k' . Since $u = r' \times k'$, $|u| = |r'| |k'| \sin \theta_{k'r'}$, where $\theta_{k'r'}$ is the angle between k' and r' . Hence, the cosine of the angle between j' and u is given by:

$$\begin{aligned} \cos \theta_{j'u} &= \frac{u_z}{|u|} = -\frac{1}{|u|} r'_y k'_x = -\frac{|r'| |k'|}{|u|} \sin \phi_{r'} \sin \theta_{k'j'} \\ &= -\frac{\sin \theta_{k'j'} \sin \phi_{r'}}{\sin \theta_{k'r'}}, \end{aligned} \quad (11)$$

where $\phi_{r'}$ is the azimuthal angle of r' .

Using the law of cosines, it can be shown that:

$$\cos \theta_{k'r'} = \cos \theta_{k'j'} \cos \theta_{j'r'} + \sin \theta_{k'j'} \sin \theta_{j'r'} \cos \phi_{r'} = \sin \theta_{k'j'} \cos \phi_{r'}, \quad (12)$$

where we have used the fact that r' is perpendicular to j' . Therefore, combining Eqs. (11) and (12) we obtain the following expression for $\cos^2 \theta_{j'u}$:

$$\cos^2 \theta_{j'u} = \frac{\sin^2 \theta_{k'j'} (1 - \cos^2 \phi_{r'})}{1 - \sin^2 \theta_{k'j'} \cos^2 \phi_{r'}}. \quad (13)$$

In the chosen space-fixed reference frame, j' and k' do not change with rotation in the product asymptote for a given trajectory. Hence, the only variable that changes with rotation in eqn (13) is $\phi_{r'}$. Averaging over a rotational period, *i.e.* integrating eqn (13) over $\phi_{r'}$ and dividing by 2π , the average value of $\cos^2 \theta_{j'u}$ over a rotational period is given by:

$$\langle \cos^2 \theta_{j'u} \rangle_{\text{rot}} = 1 - |\cos^2 \theta_{k'j'}|^{1/2}. \quad (14)$$

Equation (14) is particularly relevant, since it relates $\theta_{j'u}$, the angle between the normal vectors to the OD rotation plane and to the three-atom plane, with $\theta_{k'j'}$. Semiclassically, $|j'| \cos \theta_{k'j'}$ is the projection of j' onto k' , that is, the product's helicity Ω' , and the right hand side of eqn (5) is recovered.

6.2 Quantum Mechanical deduction of Equation (5)

Following refs. 8,12,35, the OH molecular rotational wave function can be written as

$$|j'\Omega'\Lambda'\rangle = \left(\frac{2j'+1}{4\pi} \right)^{1/2} D_{\Omega'\Lambda'}^{j'*}(\alpha, \beta, \gamma=0), \quad (15)$$

where $D_{\Omega'\Lambda'}^{j'*}$ is the rotation matrix element and (α, β, γ) are the Euler angles which specify the orientation of the body fixed frame (BF), xyz , with respect to the space fixed (SF) frame, XYZ . The BF frame is chosen with z along the OH internuclear axis, r' , whilst the Z axis in the SF frame is chosen along the recoil velocity vector, k' . With this choice, $\beta = \theta_{k'r'}$ and $\alpha = \phi_{r'}$, which define the direction of r' in the SF frame. The angle γ is chosen to be zero, such that the line of nodes (the intersection of the XY and xy planes) is $y \equiv u$ which is perpendicular to both $z = r'$ and $Z = k'$ and, as discussed in the previous subsection, defines the normal vector to the three-body plane. The projection of the rotational angular momentum, j' , along the BF z axis is Λ' . If the open shell character of the molecule is neglected, $\Lambda' = 0$. In turn, Ω' is the projection of j' along the SF Z axis (usually m' is used to designate

the projection of \mathbf{j}' onto the SF axis, but in the present case, since \mathbf{k}' is taken as Z , it corresponds to the helicity which is commonly designated by Ω'). As discussed in refs. 8,12,13, with this choice of frames, for $\Omega' = 0$ and $j' \gg 1$, \mathbf{j}' lies along \mathbf{u} (the y axis) and xz is the rotation plane. For $\Omega' = j'$ and $j' \gg 1$, \mathbf{j}' is along the x axis, which in this case is along $-Z$ and the rotation plane is yz .

Classically, $|\mathbf{j}'|^2 \cos^2 \theta_{\mathbf{j}'\mathbf{u}}$ represents the square of the projection of \mathbf{j}' onto the \mathbf{u} vector. In QM, the equivalent magnitude would be $\langle \hat{j}'_{\mathbf{u}}^2 \rangle$, the expectation value of the square of the operator that represents the projection along \mathbf{u} . It can be shown that the expression of $\hat{j}'_{\mathbf{u}}$ is simply $-i\partial/\partial\theta_{\mathbf{k}'\mathbf{r}'}$.³⁶ Therefore

$$\begin{aligned} \langle j'_{\mathbf{u}}^2 \rangle &= \langle j' \Omega' \Lambda' | \hat{j}'_{\mathbf{u}}^2 | j' \Omega' \Lambda' \rangle = \\ &= \frac{2j'+1}{4\pi} \int_0^{2\pi} \int_{-1}^1 D_{\Omega' \Lambda'}^j(\varphi_{\mathbf{r}'}, \theta_{\mathbf{k}'\mathbf{r}'}, 0) \\ &\cdot \left(-\partial^2 / \partial \theta_{\mathbf{k}'\mathbf{r}'}^2 \right) D_{\Omega' \Lambda'}^{j'*}(\varphi_{\mathbf{r}'}, \theta_{\mathbf{k}'\mathbf{r}'}, 0) d\varphi_{\mathbf{r}'} d\cos \theta_{\mathbf{k}'\mathbf{r}'} \quad (16) \end{aligned}$$

It can be shown that the result of this integral is almost exactly

$$\langle j'_{\mathbf{u}}^2 \rangle = j'(j'+1 - \delta_{\Omega',0}) \left(1 - \left| \frac{\Omega'^2}{j'(j'+1)} \right|^{1/2} \right) \quad (17)$$

where $\delta_{\Omega',0}$ stems from the fact that for $\Omega' = 0$ the maximum value of the projection is j' . Apart from this correction, this equation is the semiclassical expression, eqn (5) of the main text.

References

- 1 R. Mariella, B. Lantsch, V. Maxson and A. Luntz, *J. Chem. Phys.*, 1978, **69**, 5411–5418.
- 2 B. Koplitz, Z. Xu, D. Baugh, S. Buelow, D. Hausler, J. Rice, H. Reisler, C. Qian, M. Noble and C. Wittig, *Faraday Discussions Chem. Soc.*, 1986, **82**, 125–148.
- 3 M. J. Bronikowski and R. N. Zare, *Chem. Phys. Lett.*, 1989, **156**, 7–13.
- 4 J. Han, X. Chem and B. Weiner, *Chem. Phys. Lett.*, 2000, **332**, 243.
- 5 S. A. Lahankar, J. Zhang, K. G. McKendrick and T. K. Minton, *Nat. Chem.*, 2013, **5**, 315.
- 6 S. A. Lahankar, J. Zhang, T. K. Minton and K. G. McKendrick, *J. Am. Chem. Soc.*, 2014, **136**, 12371–12384.
- 7 P. Andresen and E. W. Rothe, *J. Chem. Phys.*, 1985, **82**, 3634–3640.
- 8 M. H. Alexander and P. J. Dagdigian, *J. Chem. Phys.*, 1984, **80**, year.
- 9 R. Schinke, V. Engle, P. Andresen, D. Hausler and G. C. Balint-Kurti, *Phys. Rev. Lett.*, 1985, **55**, 1180.
- 10 G. C. Balint-Kurti, *J. Chem. Phys.*, 1986, **84**, 4443.
- 11 P. Andresen and R. Schinke, in *Molecular Photodissociation Dynamics*. Ed. M. N. R. Ashfold, and J. E. Baggott, Royal Society of Chemistry, London, 1987.
- 12 P. J. Dagdigian, M. H. Alexander and K. Liu, *J. Chem. Phys.*, 1989, **91**, 839.
- 13 M. H. Alexander, P. Andresen, R. Bacis, R. Bersohn, F. J.

- Comes, P. J. Dagdigian, R. N. Dixon, R. W. Field, G. W. Flynn, K. Gericke, E. R. Grant, B. J. Howard, J. R. Huber, D. S. King, J. L. Kinsey, K. Kleinermanns, K. Kuchitsu, A. C. Luntz, A. J. McCaffery, B. Pouilly, H. Reisler, S. Rosenwaks, E. W. Rothe, M. Shapiro, J. P. Simons, R. Vasudev, J. R. Wiesenfeld, C. Wittig and R. N. Zare, *J. Chem. Phys.*, 1988, **89**, 1749–1753.
- 14 M. J. Bronikowski and R. N. Zare, *Chem. Phys. Lett.*, 1990, **166**, 5–10.
- 15 R. N. Dixon, *J. Chem. Phys.*, 1995, **102**, 301.
- 16 M. Alexander, *Nat. Chem.*, 2013, **5**, 253–255.
- 17 P. Andresen and E. W. Rothe, *J. Chem. Phys.*, 1985, **82**, 3634.
- 18 T. Perkins, D. Herráez-Aguilar, G. McCrudden, J. Klos, F. J. Aoiz and M. Brouard, *J. Chem. Phys.*, 2015, **142**, 144307.
- 19 M. P. de Miranda, F. J. Aoiz, L. Bañares and V. Sáez-Rábanos, *J. Chem. Phys.*, 1999, **12**, 5368.
- 20 D. Skouteris, J. F. Castillo and D. E. Manolopoulos, *Comput. Phys. Commun.*, 2000, **133**, 128.
- 21 F. J. Aoiz, V. J. Herrero and V. Sáez-Rábanos, *J. Chem. Phys.*, 1992, **97**, 7423.
- 22 F. J. Aoiz, L. Bañares and V. J. Herrero, *J. Chem. Soc. Faraday Trans.*, 1998, **94**, 2483.
- 23 S. Rogers, D. Wang, A. Kuppermann and S. Walch, *J. Phys. Chem. A*, 2000, **104**, 2308–2325.
- 24 M. R. Hoffman and G. C. Schatz, *J. Chem. Phys.*, 2000, **113**, 9456–9465.
- 25 B. Han and Y. Zheng, *J. Comput. Chem.*, 2011, **32**, 3520–3525.
- 26 J. Zhao, *J. Chem. Phys.*, 2013, **138**, 134309.
- 27 H.-J. Werner, P. J. Knowles, R. Lindh, M. Schütz, P. Celani, T. Korona, F. R. Manby, G. Rauhut, R. D. Amos, A. Bernhardtsson, A. Berning, D. L. Cooper, M. J. O. Deegan, A. J. Dobbyn, F. Eckert, C. Hampel, G. Hetzer, A. W. Lloyd, S. J. McNicholas, W. Meyer, M. E. Mura, A. Nicklass, P. Palmieri, R. Pitzer, U. Schumann, H. Stoll, A. J. Stone, R. Tarroni, T. Thorsteinsson and M. Wang, *MOLPRO, version 2012, a package of ab initio programs*, see <http://www.molpro.net>.
- 28 H.-J. Werner, P. J. Knowles, G. Knizia, F. R. Manby and M. Schütz, *WIREs Comput. Mol. Sci.*, 2012, **2**, 242.
- 29 H.-J. Werner and P. J. Knowles, *J. Chem. Phys.*, 1985, **82**, 5053.
- 30 H.-J. Werner and P. J. Knowles, *J. Chem. Phys.*, 1988, **89**, 5803.
- 31 E. R. Davidson, *J. Comput. Phys.*, 1975, **17**, 87.
- 32 A. Aguado and M. Paniagua, *J. Chem. Phys.*, 1992, **96**, 1265–1275.
- 33 A. Aguado, C. Suarez and M. Paniagua, *J. Chem. Phys.*, 1993, **98**, 308–315.
- 34 A. Aguado, C. Tablero and M. Paniagua, *Comput. Phys. Commun.*, 1998, **108**, 259–266.
- 35 R. N. Zare, A. L. Schmeltekopf, W. J. Harrop and D. L. Albritton, *J. Mol. Spectrosc.*, 1973, **46**, 37.
- 36 R. N. Zare, *Angular Momentum*, John Wiley & Sons, 1987.